International Journal of Heat and Mass Transfer 52 (2009) 3279–3289

Contents lists available at ScienceDirect

International Journal of Heat and Mass Transfer

journal homepage: www.elsevier.com/locate/ijhmt

# Effect of pressure work and viscous dissipation in the analysis of the Rayleigh–Bénard problem

A. Barletta [a,*], D.A. Nield [b]

[a] Dipartimento di Ingegneria Energetica, Nucleare e del Controllo Ambientale (DIENCA), Università di Bologna, Viale Risorgimento 2, I-40136 Bologna, Italy
[b] Department of Engineering Science, University of Auckland, Private Bag 92019, Auckland 1142, New Zealand

ARTICLE INFO

*Article history:*
Accepted 12 December 2008
Available online 18 March 2009

*Keywords:*
Convective instability
Rayleigh–Bénard problem
Viscous dissipation
Pressure work

ABSTRACT

The classical Rayleigh–Bénard problem in an infinitely wide horizontal fluid layer with isothermal boundaries heated from below is revisited. The effects of pressure work and viscous dissipation are taken into account in the energy balance. A linear analysis is performed in order to obtain the conditions of marginal stability and the critical values of the wave number $a$ and of the Rayleigh number $Ra$ for the onset of convective rolls. Mechanical boundary conditions are considered such that the boundaries are both rigid, or both stress-free, or the upper stress-free and the lower rigid. It is shown that the critical value of $Ra$ may be significantly affected by the contribution of pressure work, mainly through the functional dependence on the Gebhart number and on a thermodynamic Rayleigh number. While the pressure work term affects the critical conditions determined through the linear analysis, the viscous dissipation term plays no role in this analysis being a higher order effect. A nonlinear analysis is performed showing that the superadiabatic Rayleigh number replaces $Ra$ in the functional dependence of the excess Nusselt number. Finally, a reasoning is proposed to show how the results obtained may be used as a test on the most appropriate formulation of the Oberbeck–Boussinesq model.



## 1. Introduction

The term "Rayleigh–Bénard problem" is the common label for the problem of the onset of convection in a horizontal fluid layer uniformly heated from below. Rayleigh [1] published an analysis on the assumption that the convection was induced by buoyancy effects. He referred to the experiments performed by Bénard [2–4], though it is now known that in the thin layers with an open top observed by Bénard the convection must have been caused primarily by surface-tension differences (the Marangoni effect) rather than buoyancy. Rayleigh employed an approximation to the basic equations of motion that he ascribed to Boussinesq [5], but Joseph [6] pointed out that the approximation had been earlier employed by Oberbeck [7]. Nowadays, the parameter whose value determines the onset of convection is called the Rayleigh number. Joseph [6] noted that this parameter appeared in a study by Lorenz [8], who also used the approximation employed by Oberbeck.

Briefly stated, the Boussinesq approximation is the assumption that all fluid properties such as viscosity and density can be taken as constants except that a buoyancy term proportional to a density difference is retained in the momentum equation; see, for example, Section 8 of Chandrasekhar [9]. This means that the fluid is taken as quasi-incompressible, the divergence of the velocity is approximated by zero in the continuity equation, and the term involving the product of the pressure and the divergence of the velocity is neglected in the thermal energy equation. In addition, a scaling argument given by Chandrasekhar [9] justifies the neglect of the viscous dissipation in the thermal energy equation. The simplified thermal energy equation was employed by Rayleigh [1], who ascribed it to Boussinesq [5].

It is obvious that for convection in the atmosphere the effect of compressibility is important. It was in this context that Jeffreys [10] considered the instability of a compressible fluid heated from below. Jeffreys employed a thermal energy equation (first derived for the thermodynamics of an elastic solid) containing a term proportional to the product of the temperature and the time derivative of the excess expansion. He concluded that the criterion for the instability of a compressible fluid could be derived from that for an incompressible fluid by replacing the applied vertical temperature gradient by the difference between that quantity and the adiabatic temperature gradient.

Subsequent investigations of "non-Boussinesq effects" in the Rayleigh–Bénard problem have concentrated on effects of temperature-dependent viscosity (see the work surveyed in Section 8.1 of [11]) and most experimental work has involved liquids rather than gases. Exceptions are the papers that we now mention.

* Corresponding author.
*E-mail addresses:* antonio.barletta@mail.ing.unibo.it (A. Barletta), d.nield@auckland.ac.nz (D.A. Nield).

0017-9310/$ - see front matter © 2009 Elsevier Ltd. All rights reserved.
doi:10.1016/j.ijheatmasstransfer.2009.02.005

**Nomenclature**

| | |
|---|---|
| $a$ | nondimensional wave number, Eqs. (31) |
| $c_p, c_v$ | specific heat at constant pressure, specific heat at constant volume |
| $C_n, \hat{C}_n$ | $n$th series coefficients, Eq. (45) |
| $\mathbb{C}, \mathbb{M}$ | nondimensional matrices with components $C_n$ and $M_{mn}$ |
| $E(y)$ | nondimensional residual, Eq. (47) |
| $D_{ij}$ | component of the nondimensional strain tensor |
| $f(y), h(y), s(y)$ | nondimensional functions, Eq. (31) |
| $F(y)$ | nondimensional function, Eq. (36) |
| $F_0, F_1, F_2$ | nondimensional coefficients, Eq. (36) |
| $g$ | modulus of gravitational acceleration |
| $\mathbf{g}$ | gravitational acceleration |
| $Ge$ | Gebhart number, Eq. (8) |
| $I_{mn}$ | nondimensional coefficients, Eq. (52) |
| $\mathbf{j}$ | unit vector in the $y$-direction |
| $k$ | thermal conductivity |
| $L$ | layer thickness |
| $Nu$ | Nusselt number, Eq. (73) |
| $p$ | nondimensional pressure, Eq. (7) |
| $P, \Pi$ | nondimensional pressure disturbance, Eqs. (15) and (65) |
| $Pr$ | Prandtl number, Eq. (8) |
| $Q$ | nondimensional function, Eq. (78) |
| $Ra$ | Rayleigh number, Eq. (8) |
| $Rs$ | superadiabatic Rayleigh number, Eq. (61) |
| $t$ | nondimensional time, Eq. (7) |
| $T$ | nondimensional temperature, Eq. (7) |
| $\bar{T}_c, \bar{T}_h$ | top and bottom boundary temperatures |
| $\mathbf{u}$ | nondimensional velocity, $\mathbf{u} = (u, v, w)$, Eq. (7) |
| $\mathbf{U}$ | nondimensional velocity disturbances, $\mathbf{U} = (U, V, W)$, Eq. (15) |
| $x, y, z$ | nondimensional coordinates, Eq. (7) |

*Greeks*

| | |
|---|---|
| $\alpha$ | thermal diffusivity |
| $\beta$ | volumetric coefficient of thermal expansion |
| $\gamma$ | nondimensional parameter, $\Lambda/Ra$ |
| $\varepsilon$ | nondimensional perturbation parameter, Eq. (15) |
| $\eta$ | exponential coefficient, Eq. (31) |
| $\theta, \Theta$ | nondimensional temperature disturbance, Eqs. (15) and (65) |
| $\Lambda$ | thermodynamic Rayleigh number, Eq. (8) |
| $\mu$ | dynamic viscosity |
| $\nu$ | kinematic viscosity |
| $\xi_1, \xi_2$ | nondimensional parameters, Eq. (38) |
| $\Xi$ | nondimensional parameter, Eq. (8) |
| $\rho$ | mass density |
| $\bar{\tau}_{xy}, \bar{\tau}_{zy}$ | viscous shear stresses on a horizontal plane, Eq. (40) |
| $\Phi$ | nondimensional parameter, Eq. (77) |
| $\psi$ | nondimensional streamfunction, Eq. (26) |

*Superscript, subscripts*

| | |
|---|---|
| - | dimensional quantity |
| $B$ | base flow |
| $cr$ | critical value |

In their experiments on the onset of convection Thompson and Sogin [12] avoided the uncertainties of optical methods, which require observations on finite-amplitude post-transition convection, by using a gas and keeping the temperature constant and varying the pressure until an increase in heat transfer indicated that convection had begun. Experimenting with three gases, they obtained for the critical Rayleigh number a value $1793 \pm 80$. It is interesting that this is marginally greater than the theoretical value of 1708, but the difference is barely of statistical significance.

The numerical investigation by Turcotte et al. [13] was primarily concerned with the influence of viscous dissipation on Bénard convection. They considered the case of a quasi-Boussinesq fluid with vanishing isothermal compressibility. In their steady-state thermal energy equation they included on the left-hand side (together with the convection term) a pressure work term that represents the adiabatic temperature gradient considered by Jeffreys [10]. On the right hand side (together with the conduction term) they had a viscous dissipation term. They considered the volume integral of this equation over a convection cell. They noted that the convection term and the conduction term make a zero contribution to this integral. They also noted that the viscous dissipation term is positive definite and represents a source. They then argued that the volume integral of the viscous dissipation term must balance the volume integral of the pressure work term. In our opinion this argument is invalid, for the following reason.

In applying the First Law of Thermodynamics to the convection cell, Turcotte et al. [13] have implicitly assumed that they have control of the heat flux over the entire boundary of the cell. However, on part of that boundary the temperature is prescribed by the boundary conditions of the Rayleigh–Bénard problem. This means that on part of the boundary they have effectively prescribed both the temperature and the heat flux. This is illegitimate. The steady-state equation is not applicable to the setting up of the Rayleigh–Bénard problem in a physical situation. The heat flux at the top and bottom boundaries adjusts to fit the prescribed temperatures at those boundaries in association with any heat source within the cell.

We conclude that the effects of viscous dissipation are not coupled in the way that Turcotte et al. [13] claim they are. Consequently a new investigation of the effects of pressure work and viscous dissipation, treated independently, is required. This is the motivation for the present paper.

Before proceeding we note that Velarde and Perez Cordon [14] pointed out that the heuristic quasi-Boussinesq approximation used by Turcotte et al. [13] is not complete because they disregarded a hydrostatic pressure contribution. We also note the work of Spiegel and Veronis [15], Spiegel [16], Giterman and Shteinberg [17,18], Zeytounian [19] and Fröhlich et al. [20] on non-Boussinesq convection, especially in deep layers. Pantokratoras [21] obtained a numerical solution of the boundary layer equations along a vertical stationary isothermal plate taking into account the viscous dissipation and the pressure work of the fluid.

This paper is concerned with convection in a Newtonian fluid. The corresponding problem in a saturated porous medium is also of interest. This has been investigated by Nield and Barletta [22].

## 2. Mathematical model

Let us consider an infinitely wide horizontal fluid layer having thickness $L$ and bounded by two rigid and impermeable planes. The lower boundary plane is maintained at temperature $\bar{T}_h$, while the upper boundary plane has a uniform temperature $\bar{T}_c < \bar{T}_h$. By assuming the validity of the Oberbeck–Boussinesq approximation, the following local balance equations hold:

$$\bar{\nabla}\cdot\bar{\mathbf{u}}=0, \tag{1}$$

$$\rho\left(\frac{\partial\bar{\mathbf{u}}}{\partial\bar{t}}+\bar{\mathbf{u}}\cdot\bar{\nabla}\bar{\mathbf{u}}\right)=-\bar{\nabla}\bar{p}+\rho\mathbf{g}-\rho\beta\mathbf{g}(\bar{T}-\bar{T}_c)+\mu\bar{\nabla}^2\bar{\mathbf{u}}, \tag{2}$$

$$\rho c_p\left(\frac{\partial\bar{T}}{\partial\bar{t}}+\bar{\mathbf{u}}\cdot\bar{\nabla}\bar{T}\right)=k\bar{\nabla}^2\bar{T}+\beta\bar{T}\left(\frac{\partial\bar{p}}{\partial\bar{t}}+\bar{\mathbf{u}}\cdot\bar{\nabla}\bar{p}\right)+2\mu\bar{D}_{ij}\bar{D}_{ij}, \tag{3}$$

where

$$\bar{D}_{ij}=\frac{1}{2}\left(\frac{\partial\bar{u}_i}{\partial\bar{x}_j}+\frac{\partial\bar{u}_j}{\partial\bar{x}_i}\right) \tag{4}$$

is the $(i,j)$-component of the strain tensor and the sum over repeated indices is implied.

In Eq. (2), the vector $\mathbf{g}=-g\mathbf{j}$ is the gravitational acceleration with modulus $g$ and parallel to the unit vector $\mathbf{j}$ in the $y$-direction orthogonal to the boundary planes. The boundary conditions are

$$\bar{y}=0:\quad \bar{\mathbf{u}}=0,\quad \bar{T}=\bar{T}_h, \tag{5}$$

$$\bar{y}=L:\quad \bar{\mathbf{u}}=0,\quad \bar{T}=\bar{T}_c. \tag{6}$$

## 3. Dimensionless equations

Up to this point, an overbar has been used to denote dimensional variables and operators. We define the dimensionless quantities

$$(\bar{x},\bar{y},\bar{z})=L(x,y,z),\quad \bar{t}=\frac{L^2}{\alpha}t,\quad \bar{\mathbf{u}}=\frac{\alpha}{L}\mathbf{u},\quad \bar{D}_{ij}=\frac{\alpha}{L^2}D_{ij},$$
$$\bar{T}=\bar{T}_c+(\bar{T}_h-\bar{T}_c)T,\quad \bar{p}=\frac{\alpha\mu}{L^2}p, \tag{7}$$

and the dimensionless parameters

$$Ra=\frac{\beta g(\bar{T}_h-\bar{T}_c)L^3}{\nu\alpha},\quad \Xi=\beta\bar{T}_c,\quad Ge=\frac{\beta gL}{c_p},$$
$$\Lambda=\frac{\beta g\bar{T}_cL^3}{\nu\alpha},\quad Pr=\frac{\nu}{\alpha}, \tag{8}$$

where $\alpha=k/(\rho c_p)$ is the thermal diffusivity and $\nu=\mu/\rho$ is the kinematic viscosity. Therefore, Eqs. (1)–(3), (5) and (6) can be rewritten as

$$\nabla\cdot\mathbf{u}=0, \tag{9}$$

$$\frac{1}{Pr}\left(\frac{\partial\mathbf{u}}{\partial t}+\mathbf{u}\cdot\nabla\mathbf{u}\right)=-\nabla p+\left(RaT-\frac{\Lambda}{\Xi}\right)\mathbf{j}+\nabla^2\mathbf{u}, \tag{10}$$

$$\frac{\partial T}{\partial t}+\mathbf{u}\cdot\nabla T=\nabla^2T+\frac{\Xi Ge}{\Lambda}\left(\frac{\Lambda}{Ra}+T\right)\left(\frac{\partial p}{\partial t}+\mathbf{u}\cdot\nabla p\right)+2\frac{Ge}{Ra}D_{ij}D_{ij}, \tag{11}$$

$$y=0:\quad \mathbf{u}=0,\quad T=1, \tag{12}$$

$$y=1:\quad \mathbf{u}=0,\quad T=0. \tag{13}$$

In Eqs. (10) and (11), $p$ denotes the actual dimensionless pressure, not the excess over a reference hydrostatic dimensionless pressure as in the classical Rayleigh–Bénard problem.

Here, $Pr$ is the Prandtl number, $Ra$ is the Rayleigh number, $Ge$ is the Gebhart number, $\Lambda$ is a thermodynamic Rayleigh number based on the reference temperature $\bar{T}_c$. Eq. (11) reveals that the limit $Ge\to 0$ corresponds to negligible effects of pressure work and viscous dissipation, i.e., to the classical Rayleigh–Bénard problem. It must be mentioned that the Gebhart number coincides with the *dissipation number*, $Di$, introduced in Turcotte et al. [13].

## 4. Basic solution

A basic solution of Eqs. (9)–(13) is such that the fluid is at rest with stationary temperature and pressure distributions, namely

$$\mathbf{u}_B=0,\quad T_B=1-y,\quad p_B=Ra\,y\left(1-\frac{\Lambda}{\Xi Ra}-\frac{y}{2}\right). \tag{14}$$

We point out that, since $p_B$ is defined up to an arbitrary additive constant, this constant can be fixed so that $p_B=0$ at $y=0$.

## 5. Linear disturbance equations

Starting from the basic solution (14), one can define small perturbations of the velocity, temperature and pressure fields,

$$\mathbf{u}=\mathbf{u}_B+\varepsilon\mathbf{U},\quad T=T_B+\varepsilon\theta,\quad p=p_B+\varepsilon P, \tag{15}$$

where $\varepsilon$ is an arbitrary small perturbation parameter and $\mathbf{U}=(U,V,W)$.

On substituting Eqs. (14) and (15) into Eqs. (9)–(13) and neglecting terms of order $\varepsilon^2$, one obtains

$$\nabla\cdot\mathbf{U}=0, \tag{16}$$

$$\frac{1}{Pr}\frac{\partial\mathbf{U}}{\partial t}=-\nabla P+Ra\,\theta\mathbf{j}+\nabla^2\mathbf{U}, \tag{17}$$

$$\frac{\partial\theta}{\partial t}-V=\nabla^2\theta+\frac{\Xi Ge}{\Lambda}\left(\frac{\Lambda}{Ra}+1-y\right)\left[\frac{\partial P}{\partial t}+Ra\left(1-\frac{\Lambda}{\Xi Ra}-y\right)V\right], \tag{18}$$

$$y=0,1:\quad \mathbf{U}=0,\quad \theta=0. \tag{19}$$

Eq. (18) reveals that, in the linearization of the energy balance, there is no effect of the viscous dissipation term, as this term produces a contribution of order $\varepsilon^2$. On the other hand, there is a contribution of order $\varepsilon$ of the pressure work. This contribution results in the term proportional to $Ge$ on the right-hand side of Eq. (18).

### 5.1. Rolls perturbation

The basic solution described by Eq. (14) is invariant under rotations around the $y$-axis. Thus, a plane wave perturbation propagating in any horizontal direction produces the same effect as a plane wave propagating along the $x$-axis. As a consequence, the analysis of roll perturbations can be formulated as a 2D-problem in the $(x,y)$-plane. One obtains

$$\frac{\partial U}{\partial x}+\frac{\partial V}{\partial y}=0, \tag{20}$$

$$\frac{1}{Pr}\frac{\partial U}{\partial t}=-\frac{\partial P}{\partial x}+\nabla^2U, \tag{21}$$

$$\frac{1}{Pr}\frac{\partial V}{\partial t}=-\frac{\partial P}{\partial y}+Ra\,\theta+\nabla^2V, \tag{22}$$

$$\frac{\partial\theta}{\partial t}-V=\nabla^2\theta+\frac{\Xi Ge}{\Lambda}\left(\frac{\Lambda}{Ra}+1-y\right)\left[\frac{\partial P}{\partial t}+Ra\left(1-\frac{\Lambda}{\Xi Ra}-y\right)V\right], \tag{23}$$

$$y=0,1:\quad U=V=0,\quad \theta=0. \tag{24}$$

Eqs. (21) and (22) can be collapsed into a single equation not containing $P$, namely

$$\left(\frac{1}{Pr}\frac{\partial}{\partial t}-\nabla^2\right)\left(\frac{\partial U}{\partial y}-\frac{\partial V}{\partial x}\right)=-Ra\frac{\partial\theta}{\partial x}. \tag{25}$$

Let us introduce a streamfunction $\psi(x,y)$, such that

$$U=\frac{\partial\psi}{\partial y},\quad V=-\frac{\partial\psi}{\partial x}. \tag{26}$$

Then Eq. (20) is identically satisfied, while Eqs. (21), (25), (23) and (24) can be rewritten, respectively, as

$$\left(\frac{1}{Pr}\frac{\partial}{\partial t}-\nabla^2\right)\frac{\partial\psi}{\partial y}=-\frac{\partial P}{\partial x}, \tag{27}$$

$$\left(\frac{1}{Pr}\frac{\partial}{\partial t}-\nabla^2\right)\nabla^2\psi=-Ra\frac{\partial\theta}{\partial x}, \tag{28}$$

$$\frac{\partial\theta}{\partial t}+\frac{\partial\psi}{\partial x}=\nabla^2\theta+\frac{\Xi Ge}{\Lambda}\left(\frac{\Lambda}{Ra}+1-y\right)\left[\frac{\partial P}{\partial t}-Ra\left(1-\frac{\Lambda}{\Xi Ra}-y\right)\frac{\partial\psi}{\partial x}\right], \tag{29}$$

$$y=0,1: \quad \psi=\frac{\partial\psi}{\partial y}=0, \quad \theta=0. \tag{30}$$

We look for solutions of Eqs. (27)–(30) having the form

$$\psi=f(y)e^{\eta t}\sin(ax), \quad P=s(y)e^{\eta t}\cos(ax), \quad \theta=h(y)e^{\eta t}\cos(ax). \tag{31}$$

When the exponential coefficient $\eta$ is positive, the wave amplitude increases in time and the basic solution is unstable. If $\eta<0$, the wave amplitude decreases in time and we have stability of the basic solution. In the following, we will be interested in determining the threshold condition $\eta=0$, i.e., the condition of marginal stability.

Substituting Eq. (31) with $\eta=0$ into Eqs. (27)–(30) yields

$$f'''(y)-a^2f'(y)+as(y)=0, \tag{32}$$

$$f''''(y)-2a^2f''(y)+a^4f(y)+aRa\,h(y)=0, \tag{33}$$

$$h''(y)-a^2h(y)-aF(y)f(y)=0, \tag{34}$$

$$y=0,1: \quad f=f'=h=0, \tag{35}$$

where the primes denote differentiation with respect to $y$ and

$$F(y)=1+\frac{\Xi Ge Ra}{\Lambda}\left(\frac{\Lambda}{Ra}+1-y\right)\left(1-\frac{\Lambda}{\Xi Ra}-y\right)=F_0+F_1y+F_2y^2,$$

$$F_0=1+\frac{\Xi Ge Ra}{\Lambda}\left(\frac{\Lambda}{Ra}+1\right)\left(1-\frac{\Lambda}{\Xi Ra}\right),$$

$$F_1=-\frac{\Xi Ge Ra}{\Lambda}\left[2+\frac{\Lambda}{\Xi Ra}(\Xi-1)\right],$$

$$F_2=\frac{\Xi Ge Ra}{\Lambda}. \tag{36}$$

Eqs. (32)–(36) reveal that the Prandtl number has no influence in the analysis of marginal stability.

The solution of Eqs. (33)–(35) allows one to determine $f(y)$ and $h(y)$. Then, the unknown function $s(y)$ is obtained by means of Eq. (32), namely

$$s(y)=-\frac{f'''(y)-a^2f'(y)}{a}. \tag{37}$$

For any prescribed values of $a$, $Ge$, $\Xi$ and $\Lambda$, the constant $Ra$ represents the eigenvalue corresponding to the eigenfunction pair $(f,h)$ defined by the solution of Eqs. (33)–(35).

### 5.2. Numerical solution

Since Eqs. (33)–(35) are homogeneous, the solution $f$ can be arbitrarily rescaled, so that it is not restrictive to fix $f''(0)=1$. Then, one can solve Eqs. (33) and (34) under the initial condition

$$y=0: \quad f=0, \quad f'=0, \quad f''=1, \quad f'''=\xi_1, \quad h=0, \quad h'=\xi_2, \tag{38}$$

where $\xi_1$ and $\xi_2$ are unknown parameters to be determined, together with the eigenvalue $Ra$, by means of the constraint conditions at $y=1$, namely

$$f(1)=0, \quad f'(1)=0, \quad h(1)=0. \tag{39}$$

The eigenvalue problem Eqs. (33)–(35) can be solved numerically by employing function `NDSolve` within the software package *Mathematica 6.0* (© Wolfram, Inc.). This function allows one to solve numerically an initial value problem defined by a system of ordinary differential equations.

Eqs. (33) and (34) are subject to the initial condition Eq. (38). Then, the eigenvalue $Ra$ and the constants $\xi_1$ and $\xi_2$ are determined by solving the constraints, Eq. (39), numerically using the function `FindRoot`. The numerical solution has been performed by selecting the explicit Runge–Kutta method among those built in `NDSolve` [24].

### 5.3. Linear stability

Tables 1–3 show the critical values of $a$, $Ra$, $\xi_1$ and $\xi_2$ for $\Xi=1$, referring to $\Lambda=5000$ (Table 1), to $\Lambda=10^4$ (Table 2) and to $\Lambda=10^6$ (Table 3). The main result obtained from these tables is that $Ra_{cr}$ is an increasing function of $Ge$. Physically, this means that the critical value of $Ra$ leading to rolls instabilities is increased if the pressure work is taken into account. In other words, the effect of pressure work is stabilizing. Tables 1–3 allow one to infer that the effect of the pressure work term on the value of $Ra_{cr}$ is more and more

**Table 1**
Rigid boundaries: critical values of $a$, $Ra$, $\xi_1$ and $\xi_2$, with $\Xi=1$ and $\Lambda=5000$.

| $Ge$ | $a$ | $Ra$ | $\xi_1$ | $\xi_2$ |
|---|---|---|---|---|
| 0 | 3.116 | 1707.76 | −6.467 | −0.012104 |
| $10^{-8}$ | 3.116 | 1707.76 | −6.467 | −0.012104 |
| $10^{-4}$ | 3.116 | 1708.25 | −6.467 | −0.012100 |
| $10^{-3}$ | 3.116 | 1712.60 | −6.467 | −0.012070 |
| $10^{-2}$ | 3.116 | 1756.06 | −6.468 | −0.011776 |
| $10^{-1}$ | 3.116 | 2181.48 | −6.473 | −0.009535 |
| 1/4 | 3.117 | 2845.81 | −6.492 | −0.007456 |
| 1/2 | 3.119 | 3805.65 | −6.554 | −0.005941 |
| 3/4 | 3.126 | 4578.64 | −6.656 | −0.005417 |
| 1 | 3.144 | 5188.63 | −6.794 | −0.005317 |

**Table 2**
Rigid boundaries: critical values of $a$, $Ra$, $\xi_1$ and $\xi_2$, with $\Xi=1$ and $\Lambda=10^4$.

| $Ge$ | $a$ | $Ra$ | $\xi_1$ | $\xi_2$ |
|---|---|---|---|---|
| 0 | 3.116 | 1707.76 | −6.467 | −0.012104 |
| $10^{-8}$ | 3.116 | 1707.76 | −6.467 | −0.012104 |
| $10^{-4}$ | 3.116 | 1708.75 | −6.467 | −0.012097 |
| $10^{-3}$ | 3.116 | 1717.68 | −6.467 | −0.012034 |
| $10^{-2}$ | 3.116 | 1806.86 | −6.468 | −0.011442 |
| $10^{-1}$ | 3.116 | 2687.82 | −6.472 | −0.007727 |
| 1/4 | 3.117 | 4092.02 | −6.492 | −0.005190 |
| 1/2 | 3.120 | 6177.07 | −6.581 | −0.003757 |
| 3/4 | 3.137 | 7893.24 | −6.750 | −0.003385 |
| 1 | 3.186 | 9257.65 | −6.999 | −0.003387 |

**Table 3**
Rigid boundaries: critical values of $a$, $Ra$, $\xi_1$ and $\xi_2$, with $\Xi=1$ and $\Lambda=10^6$.

| $Ge$ | $a$ | $Ra$ | $\xi_1$ | $\xi_2$ |
|---|---|---|---|---|
| 0 | 3.116 | 1707.76 | −6.467 | −0.012104 |
| $10^{-8}$ | 3.116 | 1707.77 | −6.467 | −0.012104 |
| $10^{-4}$ | 3.116 | 1807.76 | −6.467 | −0.011434 |
| $10^{-3}$ | 3.116 | 2707.76 | −6.467 | −0.007634 |
| $2\times10^{-3}$ | 3.116 | 3707.75 | −6.467 | −0.005575 |
| $5\times10^{-3}$ | 3.116 | 6707.70 | −6.467 | −0.003082 |
| $7\times10^{-3}$ | 3.116 | 8707.62 | −6.467 | −0.002374 |
| $10^{-2}$ | 3.116 | 11707.4 | −6.467 | −0.001766 |
| $2\times10^{-2}$ | 3.116 | 21705.2 | −6.468 | −0.000953 |
| $5\times10^{-2}$ | 3.116 | 51670.9 | −6.475 | −0.000404 |
| $7\times10^{-2}$ | 3.117 | 71608.5 | −6.489 | −0.000295 |
| $10^{-1}$ | 3.118 | 101423 | −6.529 | −0.000217 |

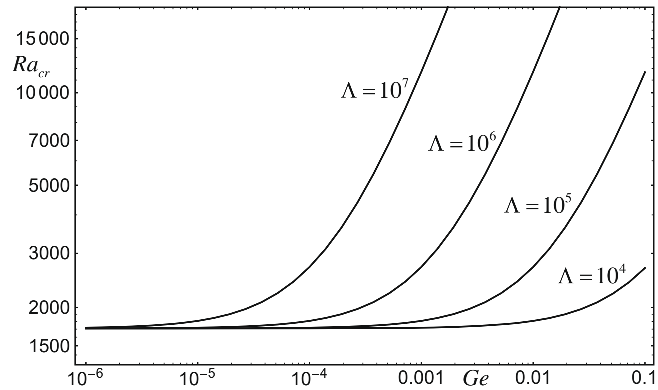


**Fig. 1.** Rigid boundaries: plots of $Ra_{cr}$ versus $Ge$ for $\Xi = 1$ and different values of $\Lambda$.

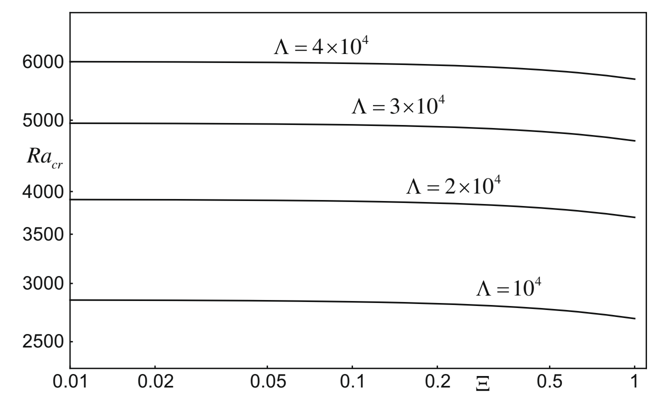


**Fig. 2.** Rigid boundaries: plots of $Ra_{cr}$ versus $\Xi$ for $Ge = 0.1$ and different values of $\Lambda$.

intense as the thermodynamic Rayleigh number $\Lambda$ increases. In particular, one can postulate, from the results collected in Tables 1–3, that $Ra_{cr}$ for sufficiently small values of $Ge$ can be approximately computed by adding to 1707.76, obtained for $Ge \to 0$, a correction term given by the product $Ge\,\Lambda$. This feature is particularly evident in Table 3. A theoretical foundation for this form of the correction term has been deduced in the case of thermally-induced instabilities in a fluid saturated porous medium bounded by isothermal impermeable planes [22]. In Section 6.1, a proof of the conjecture regarding the effect of pressure work on the value of $Ra_{cr}$ is found with reference to the case of two stress-free boundaries. Tables 1–3 also show that the change of $a_{cr}$ with $Ge$ is definitely a minor one, unless one reaches very high values of $Ge$. Fig. 1 displays plots of $Ra_{cr}$ versus $Ge$ for different values of $\Lambda$. This figure confirms that the change of $Ra_{cr}$ with $Ge$ becomes steeper and steeper as $\Lambda$ increases. Fig. 2 shows that $Ra_{cr}$ has a weak dependence on the parameter $\Xi$ if compared with the dependence on $\Lambda$. The streamlines $\psi = constant$ and the isotherms $\theta = constant$ are displayed in Fig. 3 with reference to the critical conditions, $a = a_{cr}$ and $Ra = Ra_{cr}$, for $\Lambda = 10^4, \Xi = 1$ and two extremely different cases, $Ge = 0$ and $Ge = 1$. This figure allows a comparison between the case of negligible pressure work, $Ge = 0$, and a case with an extremely intense pressure work, $Ge = 1$. The major effect of the pressure work contribution is in the modification of the isotherms. In fact, by comparing the cases $Ge = 0$ and $Ge = 1$, one may notice for $Ge = 1$ a heat flux on the bottom boundary higher than the heat flux on the top boundary. This evident asymmetry is accompanied by a less evident downward shift of the streamline rolls.

## 6. Stress-free boundaries

As is well known [23], the original Rayleigh study of 1916 [1] was referred to the case of stress-free boundaries. This means that, instead of the no-slip conditions $\bar{\mathbf{u}} = 0$ invoked in the case of rigid boundaries examined in the preceding sections, one has the boundary condition

$$\bar{v} = 0, \quad \bar{\tau}_{xy} = \mu \frac{\partial \bar{u}}{\partial \bar{y}} = 0, \quad \bar{\tau}_{zy} = \mu \frac{\partial \bar{w}}{\partial \bar{y}} = 0, \tag{40}$$

where $\bar{\tau}_{xy}$ and $\bar{\tau}_{zy}$ are the viscous shear stresses on a horizontal plane. This scheme implies that the stress-free boundary is assumed to be not affected by deformation effects, i.e., gravity waves or capillary ripples [23].

One may consider both horizontal boundaries subject to the boundary condition, Eq. (40), namely Rayleigh's problem, or just one of them. One has two main cases:

1. both stress-free boundaries, namely

$$\begin{aligned} y = 0: &\quad \frac{\partial u}{\partial y} = 0, \quad v = 0, \quad \frac{\partial w}{\partial y} = 0, \quad T = 1, \\ y = 1: &\quad \frac{\partial u}{\partial y} = 0, \quad v = 0, \quad \frac{\partial w}{\partial y} = 0, \quad T = 0; \end{aligned} \tag{41}$$

2. upper stress-free boundary and lower rigid boundary, namely

$$\begin{aligned} y = 0: &\quad \mathbf{u} = 0, \quad T = 1, \\ y = 1: &\quad \frac{\partial u}{\partial y} = 0, \quad v = 0, \quad \frac{\partial w}{\partial y} = 0, \quad T = 0. \end{aligned} \tag{42}$$

In both these cases, the basic solution, Eq. (14), is not influenced by the different boundary conditions. The reasoning behind the formulation of Eqs. (32)–(34) is left unchanged by the different boundary conditions, while Eq. (35) is either replaced by

$$y = 0, 1: \quad f = f'' = h = 0, \tag{43}$$

for both stress-free boundaries, or by

$$\begin{aligned} y = 0: &\quad f = f' = h = 0, \\ y = 1: &\quad f = f'' = h = 0, \end{aligned} \tag{44}$$

for upper stress-free boundary and lower rigid boundary.

### 6.1. Both boundaries stress-free

In this case, an approximate analytical solution based on the method of weighted residuals can be found, by assuming

$$f(y) = \sum_{n=1}^{N} C_n \sin(n\pi y), \quad h(y) = \sum_{n=1}^{N} \hat{C}_n \sin(n\pi y), \tag{45}$$

where $C_n$ and $\hat{C}_n$ are yet unknown coefficients. Substituting Eq. (45) into Eq. (33) and using the orthogonality of functions $\sin(n\pi y)$, one obtains

$$\hat{C}_n = -(n^2\pi^2 + a^2)^2 \frac{C_n}{a\,Ra}. \tag{46}$$

On account of Eq. (46), substitution of Eq. (45) into Eq. (34) yields the residual

$$E(y) = \frac{1}{a\,Ra} \sum_{n=1}^{N} C_n [(n^2\pi^2 + a^2)^3 - a^2\,Ra\,F(y)] \sin(n\pi y). \tag{47}$$

We prescribe the orthogonality between the residual $E(y)$ and the weight functions $\sin(n\pi y)$ with $1 \leqslant n \leqslant N$, namely

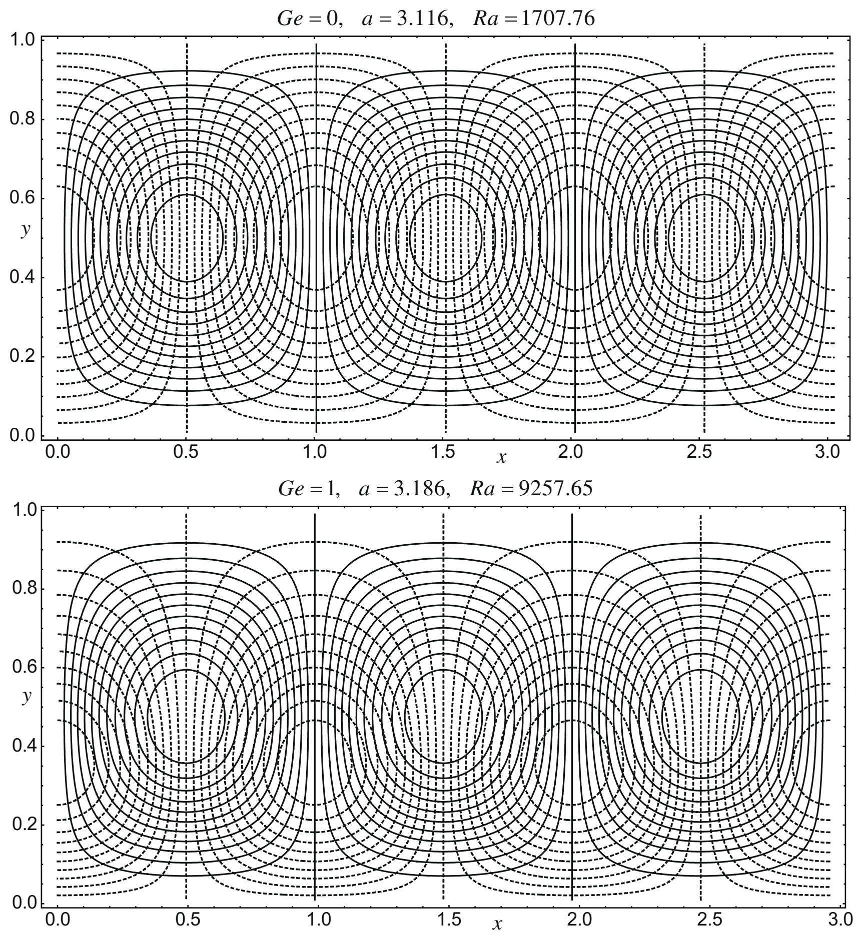


**Fig. 3.** Rigid boundaries: streamlines $\psi = constant$ (solid lines) and isotherms $\theta = constant$ (dashed lines) with $\Lambda = 10^4, \Xi = 1$ under critical conditions for $Ge = 0$ (upper frame) and $Ge = 1$ (lower frame).

$$\int_0^1 E(y)\sin(n\pi y)dy = 0, \quad 1 \leqslant n \leqslant N. \tag{48}$$

Thus, we obtain the algebraic linear system

$$\mathbb{M}\mathbb{C} = 0, \tag{49}$$

where $\mathbb{M}$ is a $N \times N$ square matrix with elements

$$M_{mn} = (n^2\pi^2 + a^2)^3\delta_{mn} - a^2 Ra\, I_{mn}, \tag{50}$$

$\mathbb{C}$ is the $N$-dimensional vector of the coefficients $C_n, \delta_{mn}$ is the $N$-dimensional Kronecker's delta and $I_{mn}$ are the coefficients,

$$I_{mn} = 2\int_0^1 F(y)\sin(m\pi y)\sin(n\pi y)dy. \tag{51}$$

One obtains the following expressions:

$$I_{nn} = 1 + \frac{Ge}{6}\left[\frac{\Xi Ra}{\Lambda}\left(2 - \frac{3}{n^2\pi^2}\right) - 3(1 - \Xi) - \frac{6\Lambda}{Ra}\right],$$
$$I_{mn} = 4mn\,Ge\frac{[1 - (-1)^{m+n}]\Lambda(\Xi - 1) + 2Ra\,\Xi}{(m^2 - n^2)^2\pi^2\Lambda}, \quad m \neq n. \tag{52}$$

The linear system, Eq. (49), admits nonvanishing solutions $\mathbb{C}$ provided that

$$\det \mathbb{M} = 0. \tag{53}$$

The eigenvalue $Ra$ can be determined by the solution of Eq. (53).

In the limit $Ge \to 0$, Eq. (53) can be easily solved. In this limit, the effect of the pressure work becomes negligible, Eqs. (37) and (38) imply that the matrix $\mathbb{M}$ becomes diagonal and Eq. (53) can be rewritten as

$$\prod_{n=1}^{N}[(n^2\pi^2 + a^2)^3 - a^2 Ra] = 0. \tag{54}$$

Eq. (54) is fulfilled if

$$Ra = \frac{(n^2\pi^2 + a^2)^3}{a^2}, \tag{55}$$

for some positive integer $n$. Each $n$ defines a different mode of instability, the most effective being the lowest one, i.e., $n = 1$. This mode yields a minimum of function $Ra(a)$ for

$$a = a_{cr} = \frac{\pi}{\sqrt{2}} \cong 2.22144, \tag{56}$$

such that

$$Ra(a_{cr}) = Ra_{cr} = \frac{27\pi^4}{4} \cong 657.511. \tag{57}$$

Eqs. (56) and (57) are consistent with the well-known result originally obtained by Rayleigh and reported, for instance, in [23].

The limit $Ge \to 0$ is the only case such that the method of weighted residuals yields an exact solution. This is due to the matrix $\mathbb{M}$ being diagonal in this case, thus preventing an entanglement of different $n$-modes in the evaluation of the determinant.

The lowest order approximation is obtained by setting $N = 1$. In this case, the matrix $\mathbb{M}$ has just one element, $M_{11}$. Therefore, from Eqs. (50)–(52), we can see that Eq. (53) is fulfilled with

$$\frac{(\pi^2+a^2)^3}{a^2} - Ra - \frac{Ge\,Ra}{6}\left[\frac{\Xi\,Ra}{\Lambda}\left(2-\frac{3}{\pi^2}\right) - 3(1-\Xi) - \frac{6\Lambda}{Ra}\right] = 0. \quad (58)$$

Eq. (58) defines the marginal stability relation $(a, Ra)$ in an implicit form. In general, Eq. (58) has two roots. However, in the limiting case $\Lambda/Ra \gg 1$, Eq. (58) yields a unique root, namely

$$Ra = \frac{(\pi^2+a^2)^3}{a^2} + Ge\,\Lambda. \quad (59)$$

Seeking the minimum of $Ra$ as a function of $a$ as given in Eq. (59), we find the critical values

$$a_{cr} = \frac{\pi}{\sqrt{2}}, \quad Ra_{cr} = \frac{27\pi^4}{4} + Ge\,\Lambda. \quad (60)$$

Eq. (60) is a proof, referred to the case of stress-free boundaries, of the conjecture described in Section 5.4. Eq. (60) shows that the classical result, Eq. (57), is recovered by replacing $Ra$ with the *superadiabatic Rayleigh number*

$$Rs = Ra - Ge\,\Lambda. \quad (61)$$

It may be noted that $Rs$ is obtained from $Ra$ by replacing the applied temperature gradient by the difference between that quantity and the adiabatic temperature gradient $\beta g \bar{T}_c / c_p$. This is in accord with the result of Jeffreys [10] mentioned in the Introduction.

In the approximation $N = 1$, the critical values $a_{cr}$ and $Ra_{cr}$ can be obtained by differentiating Eq. (58) with respect to $a$ and prescribing $dRa/da = 0$. We find $a_{cr} = \pi/\sqrt{2}$ and, correspondingly, a unique positive root of Eq. (58),

$$Ra_{cr} = \frac{3\pi^2\Lambda[Ge(1-\Xi)-2]}{2Ge(2\pi^2-3)\Xi} + \frac{\pi\sqrt{3\Lambda}}{2Ge(2\pi^2-3)\Xi} \times \left\{3\pi^2\Lambda[Ge(\Xi-1)+2]^2 + 2Ge(2\pi^2-3)(4Ge\Lambda+27\pi^4)\Xi\right\}^{1/2}. \quad (62)$$

Expanding the right-hand side of Eq. (62) in a Taylor series with respect to $Ge$ around $Ge = 0$, we obtain $Ra_{cr} = 27\pi^4/4 + O(Ge)$, so that Eq. (62) is consistent with Eq. (60).

In order to consider better approximations, i.e., $N > 1$, the solution of Eq. (53) becomes more and more complicated as $N$ increases. The evaluation of the determinant of matrix $\mathbb{M}$ can be performed by employing a software for symbolic manipulation, such as *Mathematica 6.0*. As it can be easily expected on the basis of Eqs. (50)–(52), as $N$ increases, Eq. (53) becomes an algebraic equation of increasing degree in the unknown $Ra$. This means that, as $N$ increases, several marginal stability curves will appear on the plane $(a, Ra)$. Among these non-intersecting curves, the most interesting is the lower one as it represents the boundary between the stable and the unstable region in the parametric plane $(a, Ra)$.

**Table 4**
Stress-free boundaries: critical values of $a$ and $Ra$, with $\Xi = 1$ and $\Lambda = 10^4$. Data refer to BSF = *both boundaries stress-free* or USF = *upper boundary stress-free and lower boundary rigid*.

| *Ge* | BSF | | USF | |
|---|---|---|---|---|
| | *a* | *Ra* | *a* | *Ra* |
| 0 | 2.221 | 657.511 | 2.682 | 1100.65 |
| $10^{-8}$ | 2.221 | 657.511 | 2.682 | 1100.65 |
| $10^{-4}$ | 2.221 | 658.510 | 2.682 | 1101.65 |
| $10^{-3}$ | 2.221 | 667.499 | 2.682 | 1110.62 |
| $10^{-2}$ | 2.221 | 757.349 | 2.682 | 1200.30 |
| $10^{-1}$ | 2.221 | 1649.82 | 2.683 | 2090.19 |
| 1/4 | 2.222 | 3089.93 | 2.684 | 3526.10 |
| 1/2 | 2.228 | 5262.43 | 2.694 | 5707.24 |
| 3/4 | 2.270 | 7070.28 | 2.730 | 7552.10 |
| 1 | 2.410 | 8505.45 | 2.828 | 9047.81 |

The results of the approximate analytical solution based on the method of weighted residuals are validated by the same numerical procedure described in Section 5.3. This time the initial conditions are given by

$$y = 0: \quad f = 0, \quad f' = 1, \quad f'' = 0, \quad f''' = \xi_1, \quad h = 0, \quad h' = \xi_2, \quad (63)$$

instead of Eq. (38). The definition of the parameters $\xi_1$ and $\xi_2$ obviously remains unchanged. These parameters, together with the eigenvalue $Ra$, are determined by solving the constraints

$$f(1) = 0, \quad f''(1) = 0, \quad h(1) = 0, \quad (64)$$

instead of Eq. (39). Values of $a_{cr}$ and $Ra_{cr}$ referring to $\Xi = 1$ and $\Lambda = 10^4$ are reported in Table 4 for different $Ge$. Again the change of $a_{cr}$ is very small, while the change of $Ra_{cr}$ is more apparent especially when $Ge$ becomes very large. Fig. 4 displays plots of $Ra_{cr}$ versus $Ge$ for values of $\Lambda$ increasing from $10^4$ to $10^7$. Data obtained numerically by the explicit Runge–Kutta numerical scheme are compared with those evaluated by means of the approximate formula (62). The comparison reveals a fair agreement in the whole range displayed in Fig. 4. The dependence of $Ra_{cr}$ on parameter $\Xi$ is very weak as it is shown in Fig. 5 and as it has been already pointed out in the case of rigid boundaries. Fig. 6 displays the streamlines $\psi = constant$ and the isotherms $\theta = constant$ for critical conditions, $a = a_{cr}$ and $Ra = Ra_{cr}$, with $\Lambda = 10^4$, $\Xi = 1$ and $Ge = 0, 1$. With respect to the similar Fig. 3, the effect of the pressure work contribution yields an even stronger modification of the isotherms. For $Ge = 1$, one has a marked asymmetry between the high heat flux

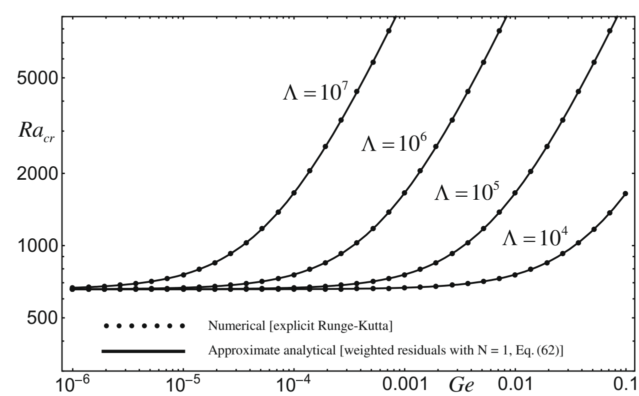


**Fig. 4.** Both boundaries stress-free: plots of $Ra_{cr}$ versus $Ge$ for $\Xi = 1$ and different values of $\Lambda$.

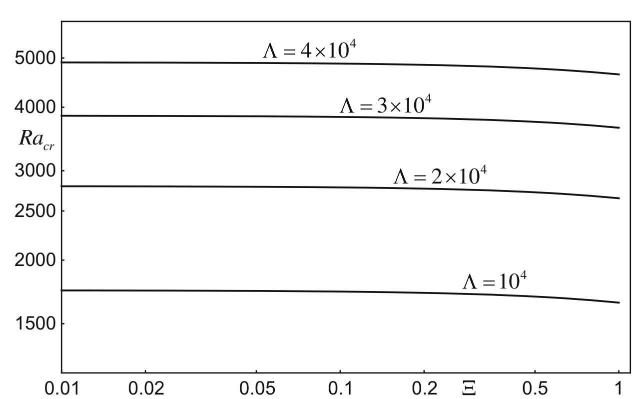


**Fig. 5.** Both boundaries stress-free: plots of $Ra_{cr}$ versus $\Xi$ for $Ge = 0.1$ and different values of $\Lambda$.

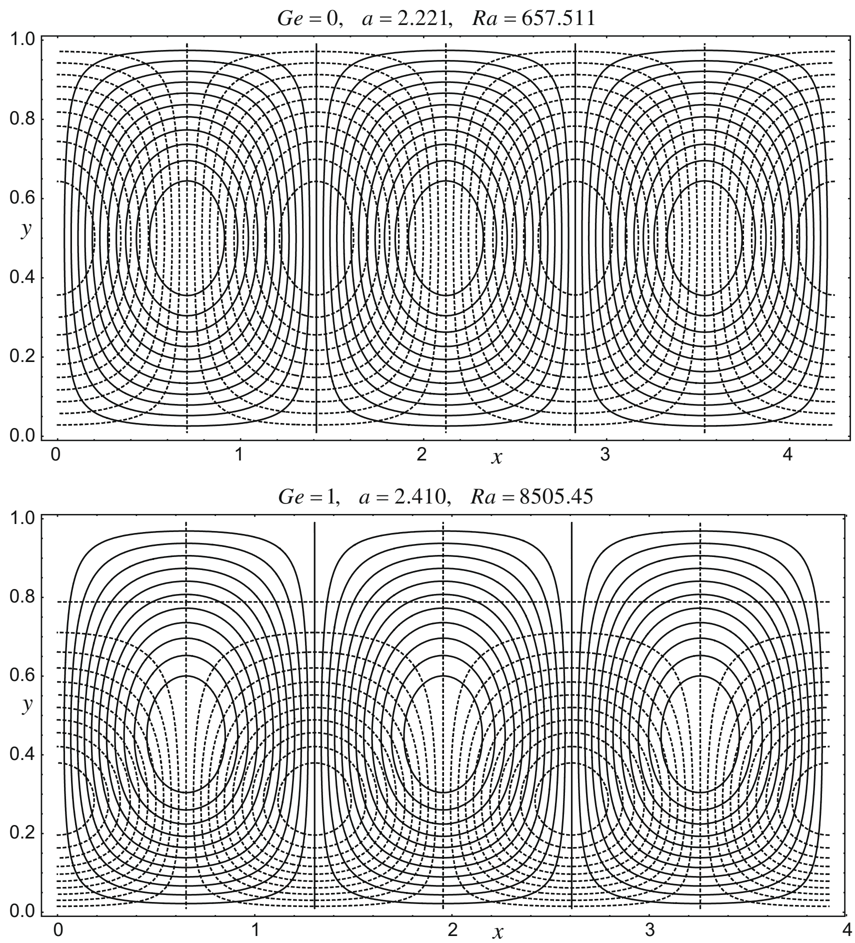


**Fig. 6.** Both boundaries stress-free: streamlines $\psi = constant$ (solid lines) and isotherms $\theta = constant$ (dashed lines) with $\Lambda = 10^4, \Xi = 1$ under critical conditions for $Ge = 0$ (upper frame) and $Ge = 1$ (lower frame).

on the bottom boundary and the almost vanishing heat flux on the top boundary. In this case ($Ge = 1$), there is also a slight downward shift of the streamline rolls.

### 6.2. Upper boundary stress-free and lower boundary rigid

The formulation of the initial value problem is identical to that expressed in Eq. (38) since the lower boundary is rigid as assumed in Section 5. What changes is the set of constraints at $y = 1$ used to determine $\xi_1, \xi_2$ and the eigenvalue *Ra*. In this case, Eq. (39) is replaced by Eq. (64). Again, the numerical solution is based on function `NDSolve` of *Mathematica 6.0*.

Table 4 displays a comparison for $\Xi = 1$ and $\Lambda = 10^4$ between the critical values of *a* and *Ra* obtained in this case with those obtained in the previous section for the case of both stress-free boundaries. In both cases, *a* and *Ra* are increasing functions of *Ge*, even if the change of *a* is definitely small. For all the values of *Ge*, the present case displays values of $a_{cr}$ and $Ra_{cr}$ intermediate

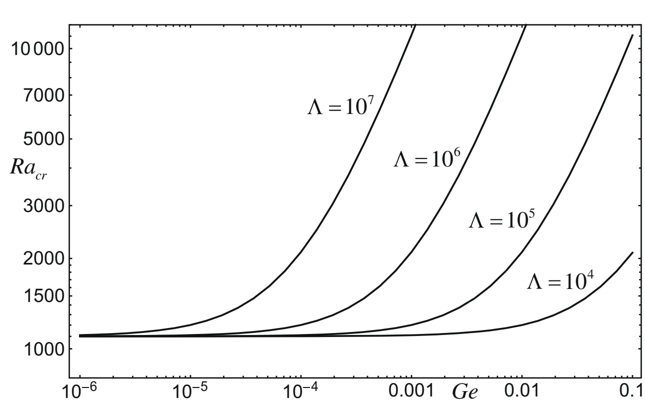


**Fig. 7.** Upper boundary stress-free and lower boundary rigid: plots of $Ra_{cr}$ versus *Ge* for $\Xi = 1$ and different values of $\Lambda$.

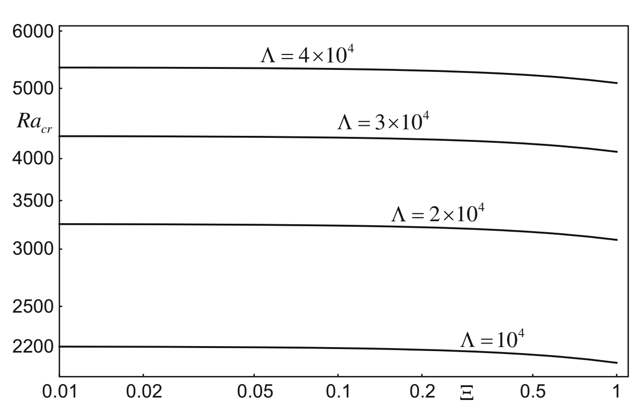


**Fig. 8.** Upper boundary stress-free and lower boundary rigid: plots of $Ra_{cr}$ versus $\Xi$ for $Ge = 0.1$ and different values of $\Lambda$.

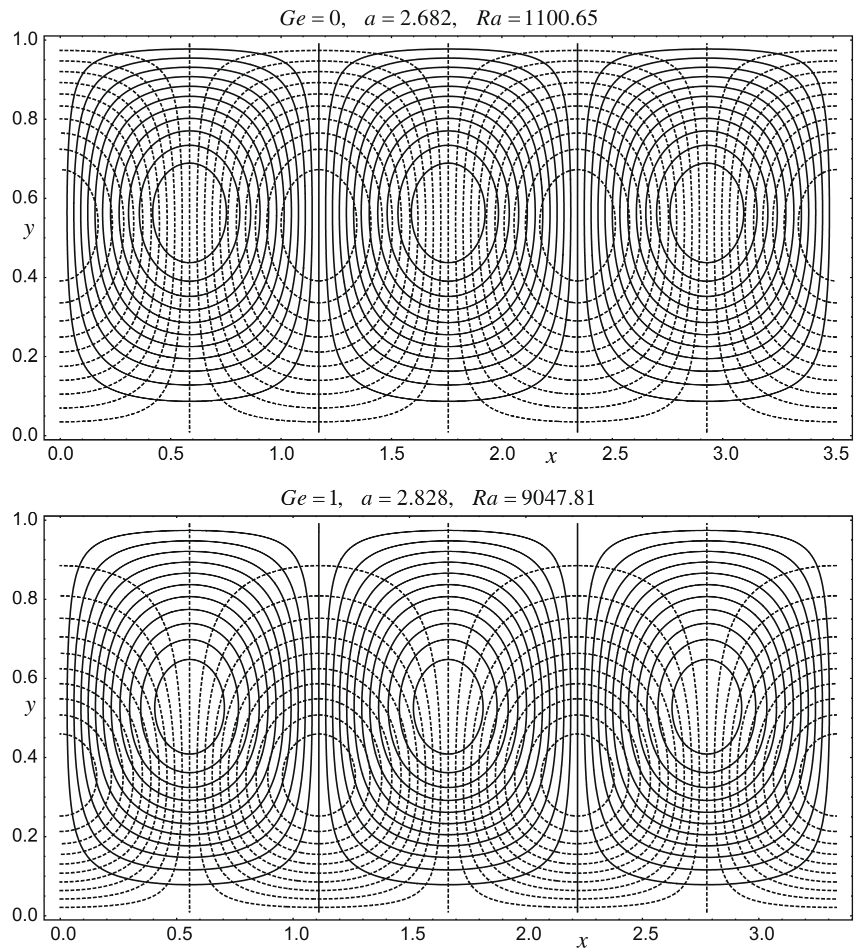


**Fig. 9.** Upper boundary stress-free and lower boundary rigid: streamlines $\psi = constant$ (solid lines) and isotherms $\theta = constant$ (dashed lines) with $\Lambda = 10^4, \Xi = 1$ under critical conditions for $Ge = 0$ (upper frame) and $Ge = 1$ (lower frame).

between the previously investigated case of both stress-free boundaries and that of both rigid boundaries. In analogy with Figs. 1, 2, 4 and 5, Figs. 7 and 8 offer a representation of the functional dependence on *Ge* (Fig. 7) and on $\Xi$ (Fig. 8). While the dependence on *Ge* can be important especially for a high value of $\Lambda$, the dependence on $\Xi$ can be considered as a minor one, as in the previously considered cases. The streamlines and the isotherms for critical conditions with $\Lambda = 10^4$, $\Xi = 1$ and $Ge = 0, 1$ are shown in Fig. 9. Unlike in Figs. 3 and 6, here we have an asymmetry in the mechanical boundary conditions at $y = 0, 1$ inducing an asymmetry of the isotherms and, even more evident, of the streamlines also in the absence of any pressure work effect ($Ge = 0$). As in Figs. 3 and 6, this effect yields a marked increase of the heat flux at the bottom boundary in the case $Ge = 1$. For this very high value of *Ge*, we notice also a slight downward shift of the streamline rolls leading to a more symmetric shape of the rolls with respect to the case $Ge = 0$.

## 7. Nonlinear theory

We now return to the dimensionless equations (9)–(13) and obtain equations for the finite amplitude disturbances. The analysis in this section is modeled on that presented in Busse [25]. We write

$$T = T_B + \Theta, \quad p = p_B + \Pi. \tag{65}$$

Then from Eqs. (10) and (11) we get

$$\frac{1}{Pr}\left(\frac{\partial \mathbf{u}}{\partial t} + \mathbf{u}\cdot\nabla\mathbf{u}\right) = -\nabla\Pi + Ra\,\Theta\mathbf{j} + \nabla^2\mathbf{u}, \tag{66}$$

$$\frac{\partial\Theta}{\partial t} - v + \mathbf{u}\cdot\nabla\Theta = \nabla^2\Theta + \frac{\Xi\,Ge}{\Lambda}(\gamma + 1 - y + \Theta) \times \left[Ra\left(1 - y - \frac{\gamma}{\Xi}\right)v + \frac{\partial\Pi}{\partial t} + \mathbf{u}\cdot\nabla\Pi\right] + 2\frac{\gamma\,Ge}{\Lambda}D_{ij}D_{ij}, \tag{67}$$

where $v$ is the $y$-component of $\mathbf{u}$ and $\gamma = \Lambda/Ra = \bar{T}_c/(\bar{T}_h - \bar{T}_c)$. For the steady state and for the case where $\gamma \gg 1$ and $\Xi/\gamma = \beta(\bar{T}_h - \bar{T}_c) \ll 1$, this equation reduces to

$$-v + \mathbf{u}\cdot\nabla\Theta = \nabla^2\Theta - \gamma\,Ge\,v + 2\frac{\gamma\,Ge}{\Lambda}D_{ij}D_{ij}. \tag{68}$$

Under the same assumptions, taking the scalar product of Eq. (66) with $\mathbf{u}$ and averaging over the horizontal coordinates and over a vertical section, one gets

$$Ra\langle\langle v\Theta\rangle\rangle = \langle\langle|\nabla\mathbf{u}|^2\rangle\rangle, \tag{69}$$

where

$$\langle\langle\phi\rangle\rangle = \int_0^1 \langle\phi\rangle dy \tag{70}$$

and $\langle\phi\rangle$ is the average of an arbitrary function $\phi$ with respect to the horizontal coordinates. The pressure term vanishes because the balance condition $\nabla\cdot\mathbf{u} = 0$ implies $\mathbf{u}\cdot\nabla\Pi = \nabla\cdot(\Pi\mathbf{u})$ and the integral of this vanishes as a result of the boundary conditions at $y = 0, 1$ as well as on the implicit assumption that either (i) the infinite horizontal layer is in fact an approximation to a thin finite layer with rigid vertical boundaries, or (ii) symmetric periodic conditions apply at lateral boundaries.

Multiplying Eq. (68) with $\Theta$ and averaging, one obtains after an integration by parts

$$(1 - \gamma Ge)\langle\langle v\Theta\rangle\rangle = \langle\langle|\nabla\Theta|^2\rangle\rangle - \frac{2\gamma Ge}{\Lambda}\langle\langle\Theta D_{ij}D_{ij}\rangle\rangle. \tag{71}$$

We note that the effect of pressure work is to replace $\langle\langle v\Theta\rangle\rangle$ by $(1 - \gamma Ge)\langle\langle v\Theta\rangle\rangle$ and the effect of viscous dissipation is to replace $\langle\langle|\nabla\Theta|^2\rangle\rangle$ by

$$\langle\langle|\nabla\Theta|^2\rangle\rangle - \frac{2\gamma Ge}{\Lambda}\langle\langle\Theta D_{ij}D_{ij}\rangle\rangle. \tag{72}$$

In the absence of pressure work and viscous dissipation, the standard weak nonlinear theory leads to the expression

$$Nu = 1 + \langle\langle v\Theta\rangle\rangle \tag{73}$$

for the Nusselt number $Nu$, defined as the ratio of the total heat transfer to that by conduction only. This now generalizes to

$$Nu = 1 + (1 - \gamma Ge)\langle\langle v\Theta\rangle\rangle. \tag{74}$$

One also has the relationship

$$Ra = \frac{\langle\langle|\nabla\mathbf{u}|^2\rangle\rangle\langle\langle|\nabla\Theta|^2\rangle\rangle}{\langle\langle v\Theta\rangle\rangle^2} \tag{75}$$

in the absence (from the thermal energy equation) of pressure work and viscous dissipation. Eq. (75) is obtained by multiplying the two equations (69) and (71).

The right-hand side of Eq. (75), which has been constructed so it is homogeneous in the velocity and the perturbation temperature, can be interpreted as a functional of the trial fields $\mathbf{u}$ and $\Theta$ and, as a Rayleigh quotient in a calculus of variations formulation, it forms the basis for energy stability analysis. In the present problem the energy stability limit gives the same value of $Ra$ as the linear stability limit. It turns out that the Euler equations in this formulation take the same mathematical form as the linear perturbation equations. In the present case, Eq. (75) is replaced by

$$Rs = \frac{\langle\langle|\nabla\mathbf{u}|^2\rangle\rangle\left(\langle\langle|\nabla\Theta|^2\rangle\rangle - 2\gamma Ge/\Lambda\langle\langle\Theta D_{ij}D_{ij}\rangle\rangle\right)}{\langle\langle v\Theta\rangle\rangle^2}, \tag{76}$$

where we have introduced the superadiabatic Rayleigh number, Eq. (61).

In the light of the above, we expect the following. When the Rayleigh number $Ra$ is replaced by $Rs$ the excess Nusselt number $Nu - 1$ will be reduced by a fraction

$$\Phi = \frac{2\gamma Ge}{\Lambda}\frac{\langle\langle|\nabla\mathbf{u}|^2\rangle\rangle\langle\langle\Theta D_{ij}D_{ij}\rangle\rangle}{\langle\langle|\nabla\Theta|^2\rangle\rangle}. \tag{77}$$

In other words, if the Nusselt number in the absence of pressure work and viscous dissipation is given by the functional relationship

$$Nu = 1 + Q(Ra), \tag{78}$$

then in the presence of pressure work and viscous dissipation one will have

$$Nu = 1 + (1 - \Phi)Q(Rs). \tag{79}$$

## 8. Concluding remarks

An analysis of the effects of pressure work and viscous dissipation has been performed for the onset of Rayleigh–Bénard convection within an infinitely wide horizontal fluid layer with isothermal boundaries heated from below. Being an higher order effect in this case, it has been shown that viscous dissipation plays no role in the evaluation of the critical wave number and the critical Rayleigh number for the onset of linear instabilities. On the other hand, the effect of pressure work may have an influence in the evaluation of the critical conditions for the onset of convective instabilities. A linear analysis of stability has been performed with reference to the three main velocity boundary conditions: both rigid boundaries, both boundaries stress-free, upper boundary stress-free and lower boundary rigid. In all these cases, it has been shown that the dimensionless parameters that mainly affect the critical wave number, $a_{cr}$, and the critical Rayleigh number, $Ra_{cr}$, are the Gebhart number, $Ge$, and the thermodynamic Rayleigh number, $\Lambda$. There is a third dimensionless parameter appearing in the dimensionless equations: $\Xi = \beta\bar{T}_c$. However, it has been shown that the latter parameter has a poor influence on the critical conditions for the onset of convective rolls. Reflections based on a nonlinear analysis have been also performed showing that one of the net effects of the inclusion of the viscous dissipation and of the pressure work terms in the energy balance is the replacement of the Rayleigh number with a superadiabatic Rayleigh number, $Rs = Ra - Ge\,\Lambda$, in the functional dependence of the excess Nusselt number.

One of the main conclusions of the present study is that the increase of $Ra_{cr}$ with the Gebhart number is in perfect agreement with the remarks reported in Turcotte et al. [13]. In fact, these authors perform a numerical finite-difference solution of the nonlinear governing equations including both the terms of pressure work and viscous dissipation. Turcotte et al. [13] reach the conclusion that there is a decreasing convection with increasing dissipation number, i.e., the Gebhart number $Ge$, that "can be attributed to the increase in the adiabatic temperature gradient". The latter quantity is $\beta g\bar{T}/c_p$.

It must be pointed out that we have performed the present analysis and drawn our conclusions starting from the standard Oberbeck–Boussinesq approximation. In particular, this means that we have followed most of the classical literature in this field and, among the many authors, Turcotte et al. [13]. This widely accepted formulation of the Oberbeck–Boussinesq approximation implies that we take into account the density changes with temperature only in the gravitational body force term of the momentum balance equation. Moreover, the approximation implies that we write the energy balance in the enthalpy formulation where the specific heat at constant pressure appears, as in Eq. (3). Even if widely used, the latter choice is not universally accepted. There is in fact another possible variant of the Oberbeck–Boussinesq approximation, described by Chandrasekhar [9], where the energy balance is written in the formulation involving the specific heat at constant volume, $c_v$, so that Eq. (3), by remembering that $\bar{\nabla}\cdot\bar{\mathbf{u}} = 0$, is replaced by

$$\rho c_v\left(\frac{\partial\bar{T}}{\partial\bar{t}} + \bar{\mathbf{u}}\cdot\bar{\nabla}\bar{T}\right) = k\bar{\nabla}^2\bar{T} + 2\mu\bar{D}_{ij}\bar{D}_{ij}. \tag{80}$$

We refer the reader to pages 16–18 of [9] for the details. The main differences between Eqs. (3) and (80), are that $c_p$ is replaced by $c_v$ and that no pressure work term appears in Eq. (80). This circumstance has two consequences: the thermal diffusivity used both in the expression of $Pr$ and of $Ra$ is now defined as $k/(\rho c_v)$ (Chandrasekhar calls this ratio "coefficient of thermometric conductivity"); the dimensionless equations do not contain the parameters $\Xi$ and $\Lambda$, as these parameters are due to the pressure work term that now is not present in the energy balance. The conclusion is simple: if one adopts Chandrasekhar's view of the Oberbeck–Boussinesq approximation, the predicted conditions for the onset of convective instabilities are exactly the same as in the limit $Ge \to 0$ (negligible viscous dissipation and pressure work). In fact, if one applies the usual linearization procedure, also the viscous dissipation effect is lost as an higher order effect. Then, the linear disturbances are governed by Eqs. (16) and (17), but Eq. (18) is replaced by

$$\frac{\partial \theta}{\partial t} - V = \nabla^2 \theta. \quad (81)$$

Everything goes as if one has taken the limit $Ge \to 0$ in Eq. (18). To summarize, there is an open question: is the critical value of $Ra$ influenced by $Ge$ and $\Lambda$ (we may neglect the weaker dependence on $\Xi$) or not? If the answer is "yes", then the correct statement of the energy balance in the framework of the Oberbeck–Boussinesq approximation is that based on the enthalpy formulation (involving the specific heat at constant pressure). On the contrary, if the answer is "no", then Chandrasekhar's variant of the Oberbeck–Boussinesq approximation, based on the $c_v$-formulation of the energy balance, is the correct one. We believe that the solution of this puzzle may shed a new light on the nature of the Oberbeck–Boussinesq approximation. To achieve this result, there is a great interest for new experimental investigations on the Rayleigh–Bénard system. As suggested in Figs. 1, 4 and 7, regimes with $\Lambda = 10^7$ should lead to values of $Ra_{cr}$ definitely higher than those in the limit $Ge \to 0$, even for $Ge = 10^{-5}$ or slightly smaller. There should be no practical obstacle in obtaining experimental working conditions such that $\Lambda = 10^7$ and $Ge = 10^{-5}$. This could be an interesting challenge for future experimental research on a basic issue of fluid dynamics.

## References


[1] Rayleigh, Lord, On convection currents in a horizontal layer of fluid, when the higher temperature is on the under side, Philos. Mag. 32 (1916) 529–546.

[2] H. Bénard, Tourbillons cellulaires dans une nappe liquide, Revue Gén. Sci. Pure Appl. 11 (1900) 1261–1271.

[3] H. Bénard, Tourbillons cellulaires dans une nappe liquide. Procédés mécaniques et optiques d'examen; lois numériques des phénomènes, Revue Gén. Sci. Pure Appl. 11 (1900) 1309–1328.

[4] H. Bénard, Les tourbillons cellulaires dans une nappe liquide transportant de la chaleur par convection en régime permanent, Ann. Chim. Phys. 23 (1901) 62–144.

[5] J. Boussinesq, Théorie Analytique de la Chaleur, vol. 2, Gauthier-Villars, Paris, 1903. p. 172.

[6] D.D. Joseph, Stability of Fluid Motions II, Springer, Berlin, 1976.

[7] A. Oberbeck, Über die Wärmeleitung der Flüssigkeiten bei der Berücksichtigung der Stromungen infolge von Temperaturdifferenzen, Ann. Phys. Chem. 7 (1879) 271.

[8] L. Lorenz, Über das Leitungsverm ögen der Metalle für Wärme und Elecktrizität, Ann. Phys. Chem. 13 (1881) 581.

[9] S. Chandrasekhar, Hydrodynamic and Hydromagnetic Stability, Oxford University Press, Oxford, 1961.

[10] H. Jeffreys, The instability of a compressible fluid heated below, Proc. Camb. Philos. Soc. 26 (1930) 170–172.

[11] E.L. Koschmieder, Bénard Cells and Taylor Vortices, Cambridge University Press, Cambridge, 1993.

[12] H.A. Thompson, H.H. Sogin, Experiments on the onset of thermal convection in horizontal layers of gas, J. Fluid Mech. 24 (1966) 451–479.

[13] D.L. Turcotte, A.T. Hsui, K.E. Torrance, G. Schubert, Influence of viscous dissipation on Bénard convection, J. Fluid Mech. 64 (1974) 369–374.

[14] M.G. Velarde, R. Perez Cordon, On the (non-linear) foundations of Boussinesq approximation applicable to a thin layer of fluid. (II). Viscous dissipation and large cell gap effects, J. Physique 37 (1976) 177–182.

[15] E.A. Spiegel, G. Veronis, On the Boussinesq approximation for a compressible fluid, Astrophys. J. 131 (1960) 442–447.

[16] E.A. Spiegel, Convective instability in a compressible atmosphere. I, Astrophys. J. 141 (1965) 1068–1090.

[17] M. Giterman, V. Shteinberg, Criteria of occurrence of free convection in a compressible viscous heat-conducting fluid, J. Appl. Math. Mech. 34 (1970) 305–311.

[18] M. Giterman, V. Shteinberg, Criteria for commencement of convection in a liquid close to the critical point, High Temperature 8 (1970) 754–759.

[19] R.K. Zeytounian, Bénard problem for deep convection. Rigorous derivation of approximate equations, Int. J. Eng. Sci. 27 (1989) 1361–1366.

[20] J. Fröhlich, P. Laure, R. Peyret, Large departures from the Boussinesq approximation in the Rayleigh–Bénard problem, Phys. Fluids A 4 (1992) 1355–1372.

[21] A. Pantokratoras, Effect of viscous dissipation and pressure stress work in natural convection along a vertical isothermal plate. New results, Int. J. Heat Mass Transfer 46 (2003) 4979–4983.

[22] D.A. Nield, A. Barletta, The Horton–Rogers–Lapwood problem revisited: the effect of pressure work, Transp. Porous Media 77 (2009) 143–158.

[23] C. Normand, Y. Pomeau, Convective instability: a physicist's approach, Rev. Mod. Phys. 49 (1977) 581–624.

[24] S. Wolfram, The Mathematica Book, fifth ed., Wolfram Media, Champaign, IL, 2003.

[25] F.H. Busse, Transition to turbulence in Rayleigh–Bénard convection, in: H.L. Swinney, J.P. Gollub (Eds.), Hydrodynamic Instabilities and the Transition to Turbulence, second ed., Springer, Berlin, 1985.